NUCLEAR INTERFEROMETRY WITH NEUTRONS EMITTED IN HEAVY-ION COLLISIONS

J. Pluta, B. Erazmus, R. Lednicky[1], D. Ardouin, C. Lebrun
Laboratoire de Physique Nucleaire IN2P3/CNRS et Universite de Nantes
2,rue de la Houssiniere - 44072 Nantes cedex 03 - France

P. Desesquelles
Institut des Sciences Nucleaires, IN2P3/CNRS,
et Universite Joseph Fourier,
53 Avenue des Martyrs, F-38026 Grenoble cedex, France

B. Jakobsson, B. Norén
Department of Physics, University of Lund,
Sölvegatan 14, S-223 62 Lund, Sweden

K. Miller, P. Duda
Institute of Physics, Warsaw University of Technology,
Koszykowa 75, 00-662 Warsaw, Poland

Abstract

The current status of nuclear interferometry with neutrons is briefly presented. Some basic formulae for two-nucleon interferometry are given. A short review of interferometry experiments with neutrons is followed by conclusions about future experiments. The process of neutron registration in a multimodular detection system is studied with a dedicated Monte-Carlo computer code. A simple method allowing to eliminate the effect of false coincidences is proposed. Calculations are performed for the DEMON detection system which should be well suited for this type of measurements.

Permanent address:
[1]. Institute of Physics, Czech Academy of Sciences,
Na Slovance 2, 18040 Prague 8, Czech Republic

1 Introduction

Nuclear interferometry is a specific branch of particle and nuclear physics. It links the space-time parameters of particle production and emission in the interaction process (unaccessible to direct measurements) with the measurable quantities characterizing correlations of particles emitted with small relative velocities [1,2]. The correlations arise due to three main effects: strong – and Coulomb final state interaction and quantum-statistics i.e. (anti)symmetrization of the wave function of identical (fermions)bosons. The dependence of these effects on the space-time evolution of the emission process gives information which is unaccessible by other methods [3,4,5,6,7,8].

Nuclear interferometry with neutrons has a special position in this field since neutrons are insensitive to the long-range Coulomb interaction.

First, it means that the parameters characterizing neutron emission are not distorted by the Coulomb field. Thus the neutron represents a good probe to determine the parameters of the emitting source. Neutron emission is an accompanying process in different forms of nuclear disassembly. The time scales of neutron emission are correlated with the mechanisms of nuclear disintegration. The lack of Coulomb barrier allows neutrons to "escape" from the interaction (excited) zone at smaller time intervals (excitation energies). Space-time parameters of neutron emission could thus be different than those of charged particles.

Second, the repulsive Coulomb forces wash-out the pairs of charged particles from the region of interest - that of the smallest momentum difference - which is not the case for neutrons. It makes the neutron-neutron correlation measurements more sensitive to the space-time characteristics, giving also a supplementary information about the role of Coulomb interaction by comparison to the proton-proton correlation measurements (see Fig.1). The comparison with proton-neutron correlations shows the influence of the Coulomb source on the form of the correlation function. Two-particle proton-neutron correlations can also be directly compared with the probability of deuteron formation as both are related to the final state interaction. This type of comparison can be used determine the spin state of particle sources [8].

In the first measurements of neutron-neutron correlations a positive correlation effect was observed[9]. The methodical problems due to the distortion of the measured correlation distributions have been considered in later experimental works[10,11,12,13]. In order to understand the complicated form of distortions introduced by neutron scattering, dedicated experiments have been perfomed recently[14,15].

Considering future experiments with neutron detectors the influence of the distortion effects should be estimated before choosing the detection setup. In this note we present the results of such estimations for the DEMON detector [16].

2 Basic formulae for two-nucleon interferometry

2.1 Identical noninteracting unpolarized nucleons

Let us consider two identical unpolarized nucleons (n,n), (p,p) emitted at the space-time points x_1, x_2, with 4-momenta p_1, p_2.

There are two possible spin states: S=0 (singlet) and S=1 (triplet) with populations 1/4 and 3/4 respectively. The correlation function in this case is determined by quantum statistics (Pauli principle).

$$R_{nn}(p_1,p_2) = \frac{1}{4}\langle\frac{1}{2}|e^{ip_1x_1+ip_2x_2} + e^{ip_2x_1+ip_1x_2}|^2\rangle + \frac{3}{4}\langle\frac{1}{2}|e^{ip_1x_1+ip_2x_2} - e^{ip_2x_1+ip_1x_2}|^2\rangle \quad (1)$$

The first term corresponds to the singlet (spin-antisymmetric) state, the second – to triplet (spin-symmetric) state.

The correlation function (1) can be also expressed in the form:

$$R_{nn}(p_1,p_2) = \frac{1}{4}[1 + \langle cos(qx)\rangle] + \frac{3}{4}[1 - \langle cos(qx)\rangle] = 1 - \frac{1}{2}\langle cos(qx)\rangle \quad (2)$$

where $x \equiv \{t, \vec{x}\} = x_1 - x_2$ and $q \equiv \{q_0, \vec{q}\} = p_1 - p_2$. This result was first obtained by Kopylov and Podgoretski (1972-1974) [3].

In the case of Gaussian space-time distribution of the emission points

$$W(x_i) \propto \exp(-\vec{x}_i^2/2r_0^2) \cdot \exp(-t_i^2/2\tau_0^2), \quad (3)$$

the correlation function takes the familiar form:

$$R_{nn}(p_1,p_2) = 1 - \frac{1}{2}exp(-\vec{q}^2 r_0^2 - q_0^2\tau_0^2) \quad (4)$$

2.2 Identical noninteracting polarized nucleons

In this case the populations of singlet (ρ_0) and triplet (ρ_1) states depend on the polarization vector $\vec{P}$.

$$\rho_0 = \frac{1}{4}(1 - \vec{P}_n^2) \quad (5)$$

$$\rho_1 = \frac{1}{4}(3 + \vec{P}_n^2). \quad (6)$$

The correlation function is (Lednicky-Lyuboshitz, 1981) [5]:

$$R_{nn}(p_1,p_2) = 1 - \frac{1 + \vec{P}_n^2}{2}\langle cos(qx)\rangle. \quad (7)$$

Note that completely polarized neutrons ($|\vec{P}_n^2| = 1$) can be in the spatial antisymmetric triplet state only, so that the correlation function vanishes at $p_1 \to p_2$.

2.3 Nonidentical interacting nucleons (n,p)

Due to the interaction between particles (n,p) the plane wave in the previous example is replaced by the Bethe-Salpeter amplitude:

$$e^{ip_1x_1+ip_2x_2} \rightarrow \psi^{(S)}_{p_1p_2}(x_1,x_2) = e^{ip_1x_1+ip_2x_2} + \varphi^{(S)}_{p_1p_2}(x_1,x_2), \tag{8}$$

where $\varphi^{(S)}_{p_1p_2}(x_1,x_2)$ is the scattered wave. In this case the correlation function takes the form [5]:

$$R_{np}(p_1,p_2) = \rho_0\langle|\psi^{(0)}_{p_1p_2}(x)|^2\rangle + \rho_1\langle|\psi^{(1)}_{p_1p_2}(x)|^2\rangle. \tag{9}$$

Here $\psi^{(S)}_{p_1p_2}(x)$ is obtained from Bethe-Salpeter amplitude after separation of the c.m.s. motion

$$\psi^{(S)}_{p_1p_2}(x_1,x_2) = e^{iPX}\psi^{(S)}_{p_1p_2}(x), \tag{10}$$

where $P = p_1 + p_2$ and $X = [(p_1P)x_1 + (p_2P)x_2]/P^2 \equiv \{X_0, \vec{R}\}$ is the two-particle c.m.s. 4-coordinate.

The populations of singlet and triplet spin states are:

$$\rho_0 = \frac{1}{4}(1 - \vec{P}_n\vec{P}_p) \tag{11}$$

$$\rho_0 = \frac{1}{4}(3 + \vec{P}_n\vec{P}_p) \tag{12}$$

Let us now define $x^* = (\vec{r}^*, t^*)$ in the c.m.s of the (n,p) pair. It can be shown [5] that if,

$$|t^*| \ll mr^{*2} \tag{13}$$

the approximation of equal emission time in the c.m.s of particles is valid and the amplitude $\psi^{(S)}_{p_1p_2}(x^*)$ can be replaced by the usual wave function $\psi^{(S)(+)}_{-\vec{k}^*}(\vec{r}^*)$ describing relative motion of the particles (in continous spectrum) having the asymptotics (at $r^* \rightarrow \infty$) of a superposition of the plane and diverging spherical waves

$$\psi^{(S)(+)}_{-\vec{k}^*}(\vec{r}^*) \longrightarrow e^{-i\vec{k}^*\vec{r}^*} + f^{(S)}(\vec{k}^*)\frac{e^{ik^*r^*}}{r^*}. \tag{14}$$

Note: $k^* = \sqrt{-q^2}/2$, $f^{(0)}(0) = 23.7fm, f^{(1)}(0) = -5.4fm$ and the correlation function $R(p_1 = p_2) \approx 10$ at $r_0, c\tau_0 \sim (2-3)fm$.

Condition (13) gives,

$$\tau_0 \ll mr_0\sqrt{r_0^2 + v^2\tau_0^2} \tag{15}$$

and, due to the large nucleon mass, it is usually fulfilled provided that the velocity v of the nucleon pair is not too small.

Fig.2 (from the ref. [8]) presents the singlet, triplet, and spin average correlation function for the neutron-proton system. Note that $q = k^*$ in this, and in most of other figures. (Sometimes the notation $q = 2k^*$ is used.)

2.4 Identical interacting particles

Replacing the plane waves by the Bethe-Salpeter amplitude we get

$$\begin{aligned} R_{nn}(p_1,p_2) &= \frac{1}{4}(1-\vec{P}_n^2)\langle|\frac{1}{\sqrt{2}}(\psi^{(0)}_{p_1p_2}(x)+\psi^{(0)}_{p_2p_1}(x))|^2\rangle + \\ &+ \frac{1}{4}(3+\vec{P}_n^2)\langle|\frac{1}{\sqrt{2}}(\psi^{(1)}_{p_1p_2}(x)-\psi^{(1)}_{p_2p_1}(x))|^2\rangle. \end{aligned} \tag{16}$$

Note that in the region of small relative momenta (small k^*) the s-wave strong interaction dominates and that this interaction contributes to the singlet combination only. Thus if $|\vec{P}_n| \approx 1$, the correlation due to the strong interaction vanishes (in other words, two identical nucleons in s-wave state cannot have parallel spins, i.e. be in the spin-triplet state). The first calculation of the correlation function for two nonrelativistic protons was first performed numerically by Koonin [4].

2.5 Deuteron formation rate

Assuming that the deuteron formation is dominated by the final state interaction between emitted neutrons and protons, we get the deuteron formation cross section [17,18]:

$$\sigma_d^{(1)}(P_d) = (2\pi)^3\gamma\rho_1\langle\ \psi_b^{(1)}(x)|^2\rangle \cdot \tilde{\sigma}_{np}(\frac{1}{2}P_d, \frac{1}{2}P_d) \tag{17}$$

where γ is the deuteron Lorentz factor and $\psi_b^{(1)}(x)$ is the Bethe-Salpeter amplitude describing the bound triplet state of neutron and proton. In the "equal time" approximation it coincidences with the usual deuteron wave function. $\tilde{\sigma}_{np}(p_1,p_2)$ is the production cross section of uncorrelated (n,p) pairs. It is related to the measured (n,p) production cross section $\sigma_{np}(p_1,p_2)$ through the correlation function:

$$\sigma_{np}(p_1,p_2) = R_{np}(p_1,p_2)\cdot\tilde{\sigma}_{np}(p_1,p_2). \tag{18}$$

We see that in such a model, the deuteron formation cross section is closely related to the emission of neutron-proton pairs with near-by momenta (see also refs. [8,19]).

The dependence of the deuteron formation rate on the space-time parameters are presented in the Fig.3 (from ref. [8]). Fig.4. presents a typical form of the correlation function for (n,n) pairs, calculated for different values of the time parameter τ_0.

3 Interferometry experiments with neutrons

The experimental information on interferometry measurements with neutrons is rather poor in comparison with that obtained for charged particles. This is mainly due to experimental difficulties to the measurements of neutrons. In the following list the main experimental results are presented and some specific features of different experiments are emphasized.

1. The first measurement of neutron-neutron correlations in the region of small relative momenta was performed in 1984 [9]. Seven neutron detectors, placed at different distances from the target, were used. The minimal angle between detectors was 6°. A positive correlation effect was observed for (n,n) pairs emitted in the reaction of protons with lead nuclei at 7.5 GeV/c, Fig.5. More pronounced correlations were observed for larger neutron momenta. This interesting effect was first observed in Dubna for the (p,p) pairs emitted in relativistic nuclear collisions [20,21,22]. The same effect was seen later in intermediate energy heavy-ion collisions [23]. A relation between the time parameter characterizing the emission process and the mean momentum of emitted particles was emphasized in this context [10,22].

2. Next results came from low-energy heavy-ion experiments. The correlations of neutrons were measured in the "compound-nuclear reaction": $^{18}O + {}^{26}Mg \rightarrow {}^{44}Ca$, ($E_x$ = 60 and 71 MeV) [24]. A system of four liquid scintillator counters placed at a distance of 2m from the target was used. In contrast to the previous experiment negative correlations in the region of small energy differences were observed; Fig.6. Such a result corresponds to large time intervals in the neutron emission process and indicates an absence of the final-state interaction effects.

3. First results on neutron – light-charged-particle correlations were obtained in 1990 with a system of six charged particle detectors and eight modules of NE-213 scintillator counters [25]. A clear effect of positive correlations for the (n,p) pairs emitted in $^{16}O + {}^{27}Al$ reaction at $E(^{16}O)$=215MeV was observed, showing an important role of the final-state interaction in this case (Fig.7). An attempt to measure the nuclear temperature from the relative population of deuteron excited and ground states [26] was made. The value obtained ($1.6 \pm 0.3MeV$) is much lower than expected.

4. Simultaneous measurements of two-neutron and two-proton correlations were performed in 1991 for the interactions of ^{20}Ne with C and Co targets at $30AMeV$ [11]. A system of 16 CsI detectors (EMRIC) was used to register charged particles and four liquid scintillator detectors placed at 3.5m from the target – for the detection of neutrons. A strong positive correlation effect for two-neutron system was observed (Fig.1). A model with Gaussian distribution of the emitting sources and zero value of the life-time parameter was used to describe the form of correlation function. In the frame of this approach the qualitative compatibility of the size of proton and neutron emission volumes was obtained. The dependence of the form of correlation function on the distance between detectors was observed. This effect can be attributed to different orientation of the vector of momentum difference and, in principle, it can be used to separate the space and time parameters of the particle emission process.

5. Measurements of (n,n) correlations from excited compound nucleus were performed in terms of energy-difference in the reaction $^{18}O +^{64} Ni$ at 96 MeV of

incident energy [12]. A system of three NE-213 modules was used. A negative correlations in the region of zero energy difference were observed (Fig.8), similarly to that from the ref. [24]. The role of final-state interaction was neglected in the analysis of the data.

6. More complete analysis has been performed for the reaction $^{16}O + {}^{64}Al$ at 215MeV and $^{16}O + {}^{12}C$ at 60.5 MeV [27]. A complex detection system was used including the registration of charged particles and neutrons. The data analysis was performed using two different theoretical approaches: the final-state interaction model of Koonin [4] and a semiclassical evaporation model [28,29]. An unexpected lack of correlations was obtained for the (n,p) system emitted in $^{16}O + {}^{12}C$ reaction while in the case of $^{16}O + {}^{64}Al$ at 215MeV a clear correlation effect was observed. The (n,p) correlation functions were approximated quite well by the theoretical curves but it appeared impossible to fit the (p,p) data keeping the same values of the model parameters, Fig.9.

7. The neutron-proton correlation function was measured in the reaction $^{40}Ar + {}^{191}Au$, ^{12}C, CH_2 at 30 MeV/u [13]. A well established (high statistics) weak correlation effect was observed for the Au target. More pronounced peaks were seen for light tergets; Fig.10. The results were compared with the corresponding data for (n,n) and (p,p) systems. Theoretical calculations were performed in the frame of a pure evaporative approach [7] and with the BUU dynamical model [30]. It appeared impossible to describe simultaneously the form of measured correlation function for different two-particle systems.

4 Current status and future possibilities

The experimental results obtained recently show some existing problems of nuclear interferometry but reveal also some new fields of investigation for future interferometry experiments with neutrons. Some of them are listed below.

- The emission space-time scale can be different for different particles or particle systems like deuteron.
- The Coulomb interaction between charged particles and the emitting source can change the form of the correlation function.
- A traditional approach with a static source is in many cases inadequate and should be replaced by a dynamical evolution of the emission process. Interferometry measurements can thus be used as a tool to test the validity of different dynamical models.
- The correlation function is sensitive to the spin state of two-particle system. This feature can affect the form of correlation function and can be used to determine the spin state of the source [31].

- Deuteron formation is directly related to the final state interaction in the (n,p) system. The deuteron formation rate can thus be used to find the space-time parameters in the same way as the correlation measurements. On the other hand, the (n,p) correlations can be applied to study the mechanisms of deuteron production in heavy-ion collisions.

- Methodical problems with neutron registration are particularly important in interferometry mesurements and should be properly included in the analysis of the data.

A general conclusion from the common analysis of the existing results is that despite of some problems with description of the data there are new possibilites of nuclear interferometry in simultaneous measurement of correlations for different two-particle systems like (n,n), (n,p), (p,p), (d). The "key point" of such measurements is that *different* effects participate *differently* in the correlation function for *different* types of the particle pairs:

- final state strong interaction: (p,p), (n,n) (n,p), (d);

- quantun statistics: (p,p), (n,n);

- Coulomb interaction between particles: (p,p);

- Coulomb interaction between particle and emitting source: (p,p), (p,n), (d).

Making simultaneous analysis for different two-particle systems, some selected effects can be switched off in order to isolate the effect under study. The (n,n) and (n,p) systems can be taken as an example. A Coulomb field of the emitting source which affect the (n,p) correlations is switched off in the case of the (n,n) system. It is also clear that a simultaneous description of correlation effects for different particle systems makes the constraints for any theoretical description especially strong. However, a consistent treatment of different effects in the theoretical description and in the data analysis must be carried out. Let us consider two illustrative examples.

a. Theoretical example - source-particle Coulomb interaction

The Coulomb interaction between the charged source and emitted charged particle affects strongly the value of the particle momentum. In a simple understanding, this effect should also change strongly the correlations between particles emitted with small momentum difference. Indeed, when a proton and a neutron are emitted with close momenta, the Coulomb force will "push" the proton leaving the neutron intact. Protons would be thus removed from the "critical" region [32].

To be more precise, let us take the definition of the correlation function for particles with momenta p_1 and p_2:

$$R(p_1, p_2) \sim \frac{d^6\sigma}{d^3p_1 d^3p_2} / \left(\frac{d^3\sigma}{d^3p_1} \frac{d^3\sigma}{d^3p_2} \right) . \tag{19}$$

We see that the momentum shift will be present both in numerator and denominator and thus it will be completely cancelled for uncorrelated particles. In the case of correlation between particles, the three-body treatment is indispensable in order to calculate properly the form of the correlation function in the presence of the Coulomb field. Such calculations have been performed in a classical approach [33,34]. Relatively small, but clear changes of the form of the correlation function for the proton-deuteron system have beeen obtained (Fig.11.). Similar conclusions can be drawn from the quantum calculations performed recently [35].

b. Experimental example - "cross-talk" and coincidences

Since neutrons passing the detector medium must scatter on protons or nuclei to be registered this causes some extra problems for the detection of neutrons. The multimodular detection system creates frequently many spurious signals called "cross-talk". (This effect will be considered later in details.) In the case of one-particle distributions the cross-talk effecs are usualy small or even negligible. It appeared however from dedicated measurements [14,15] and computer simulations [37] that this effect is very important in the case of coincidence measurements. For this reason the efficient neutron detectors of close geometry like TAPS or AMPHORA cannot be used for interferometry measurements with neutrons[36,37]. However, for the analysis of two-neutron correlations in the important region of small momentum difference (small relative angles), a detection system with close geometry must be used. Thus nuclear interferometry with neutrons needs very specific experimental methods. Some of them will be discussed below.

5 Interferometry measurements with neutrons

The main technique of neutron registration consists in indirect detection of the light deposited by protons or other nuclei in liquid or solid scintillators. Unfortunately, the mean free path of neutrons in the detector volume is in most cases of the same order as the size of detector and neutrons rarely deposit all the energy in the detector module. The detection efficiency (rate of detected neutrons) is usually far from a 100of light deposited is only weakly correlated with the velocity of the incoming neutron.

In interferometry measurements, involving the detection of coincident neutrons at small relative angles, a new specific instrumental problem arises due to the fact that scattering of neutrons between detectors appears frequently. Thus, when the detectors are close to each other, a neutron produced in the target can pass through several detectors. Depending on the amount of light deposited in each detector, it may, or may not, be detected. A neutron which passes successively two detectors can induce two main effects which we will call: cross-talk and diaphony [37].

a.) Cross-talk

It occurs when the neutron deposits enough light to be detected in both de-

tectors. This effect leads to an over-estimation of the total number of neutrons emitted from the target and creates spurious correlations at low relative angle. This effect is especially dangerous for the interferometry measurements.

b.) Diaphony

If the incoming neutron is detected only by the second detector, then two effects influence the measurement: the detected angles are incorrect and the energy of neutron, deduced either from the time of flight or from the light deposit, is under-estimated.

5.1 Cross-talk and coincidences - probability relations

Cross-talk effects decrease with the increasing distance between detectors. It seems therefore reasonable to keep this distance *as large as possible* in order to avoid the influence of cross-talk. Large distances between detectors correspond however to large angular intervals which is not desirable for interferometry measurements. A natural way to solve this problem is to put detectors in a large distance from the target. Does this solution decrease the cross-talk to coincidence ratio?

Let us consider a simplest example of two detectors located at the same distance from the target (Fig.12.a). In the case of fixed angle between detectors ($\alpha = const$), the dependence of the registration probability on the distance, d, between target and detectors is:

- probability of single particle registration:

$$P_s \sim 1/d^2, \tag{20}$$

- probability of coincidence registration:

$$P_c \sim P_s^2 \sim 1/d^4, \tag{21}$$

- probability of cross-talk registration:

$$P_{c-t} \sim P_s \cdot \frac{1}{h^2} \sim \frac{1}{d^2 h^2} \sim 1/d^4. \tag{22}$$

In this case the distance between detectors h is lineary related to d.

Thus the ratio of cross-talk to coincidence probability does not depend on the distance target-detectors. Keeping in mind that the probability of coincidence registration is inversely proportional to the 4th power of d, it seems much more favorable to make this distance *as small as possible* contrary to the "first-sight" estimation.

Similar conclusion can be drawn from the second example (Fig.12.b) where $h = const$. In this case the ratio of cross-talk to coincidence probability is:

$$\frac{P_{c-t}}{P_c} \sim \frac{1}{d^2 h^2} / \frac{1}{d^4} = \frac{d^2}{h^2} \sim d^2. \tag{23}$$

Here this ratio even increase as the second power of the distance target-detector because h does not depend on d.

However, the time-of flight measurements necessary for energy determination, the necessary angular resolution and the limitations in the absolute count-rate (both of singles rate and cross-talk rate) make too small distances impossible. Thus, it is *not due to cross-talk* that this distance cannot be too small in the case of interferometry measurements.

All considerations presented above are of course simplistic and Monte-Carlo simulations are necessary in order to take into account many different effects and their complicated convolution.

5.2 Monte-Carlo simulations of (n,n) correlations

In order to evaluate the influence of the detector parameters on the form of measured correlation function Monte-Carlo (M-C) simulations have been performed. In the simulation procedure all the main features of the neutron emission and detection have been taken into account. The M-C simulation program has the following structure:

5.2.1 Detector structure definition

The multimodular detection system is assumed. Each module has a cylindrical form. The following parameters are defined for each module:

- cylinder radius,
- cylinder length,
- threshold (in MeV electron equiv.),
- direction cosines of the cylinder axis,
- distance from the target.

5.2.2 Event generator

The source of neutrons is characterized by the neutron multiplicity and by energy and angular distributions of the emitted neutrons. The form of these distributions can be defined by the user. Keeping in mind that the solid angle of the considered configurations is relatively small and in order to increase the simulation efficiency, only neutrons which hit a surface of the detector are considered. Hit points are assumed to be uniformly distributed at the surface of detector. Each neutron is characterized by the direction cosines and energy.

5.2.3 MENATE - Neutron registration procedure

The process of neutron interactions in the detection system is simulated with the computer code MENATE [37], which was modified to allow for variable configuration of detector modules. For each event the simulation is developed until all participant particles leave the detector. Input data consist of:

- detector and neutron parameters (see above)
- differential cross sections for the neutron and gamma-ray interaction with the scintillator material (NE213).

The features of each neutron or gamma created in the reaction are saved in a stack. The ranges of charged particles in the material and the light deposited by each charged particle is calculated. It is assumed that charged particles are stopped in the detector walls. Output data contain all information concerning the development of the interaction process in the system of modules. Finally, the following output data are extracted for each detector:

- serial number of the primary "ancestor" neutron which has permitted the total light deposit in the detector to reach the threshold; (zero - if detector not "fired").
- time when the light deposited in the detector has reached the threshold, (zero reference point - time of the reaction in the target.)
- serial number of the interaction (from the stack) containing all other details.

5.2.4 Calculation of the correlation function

Using the momentum vectors of each generated neutron the momentum difference in the pair rest frame is calculated for each combination of registered neutrons. The weight corresponding to the momentum difference between "ancestor" neutrons is calculated using the parametrized values of the theoretical (n,n) correlation function for assumed values of the space-time parameters of the emitting source. Normalization is made so that $R = 1$ for $|\vec{p}_1 - \vec{p}_2| \rightarrow \infty$ and weight equal to one is assigned in the case of cross-talk pairs. The "measured"correlation function is calculated using the momentum differences between all "fired" detectors and the weights defined above. This procedure takes into account all the main features of the registration process:

- angular resolution due to the difference between the true hit position at the surface of detector and the position of the center of detector,
- time of flight (energy) resolution due to the fluctuation of the mean penetration depth,
- threshold of the neutron detection,

- position and energy errors due to diaphony,
- false "coincidences" due to cross-talk,
- relative probabilities of different effects corresponding to the detection probability, differential cross-sections of neutron interactions in the detectors, multiplicity, energy and angular distributions of emitted neutrons etc.

6 M-C simulations for the DEMON detector

6.1 Geometrical configurations

The simulations were performed for 96 modules of the DEMON detector [16], arranged in different geometrical configurations. The dimensions of each module are: radius 8cm, length 20cm. The neutron threshold energy is 3 MeV corresponding to an electron energy of 1.0 MeV.

The following configurations were considered:

1. Standard DEMON configuration of E236 and E240 experiments at GANIL [38] (Fig.13). (Relative angles between detectors: 22 and 13 deg. in horizontal and vertical directions respectively; distance - target-detector - 175cm).
2. First modified configuration of three rows (TEST1, Fig.14.). Detectors arranged in three rings with the angular distance between them: 5 and 8 deg.; angular distance between different systems of three detectors - 10 deg. Distance - target-detector - (150, 200, 250)cm. Angles and distances of consecutive three- detector systems change alternately.
3. Second modified configuration (TEST2) - the same as TEST1, but distances target-detector approximately doubled (350, 400, 450) cm.
4. Compact configuration (Fig.15.) - all detectors arranged in a matrix (8*12) detectors with the angular distance of 1.2 deg. and a distance target-detectors - 1000cm. The distance between centers of detectors: 20cm.
5. The same geometrical configuration as the TEST1 but with smaller energy threshold of 0.1 MeV electron equivalent energy (TEST1,a).

6.2 Neutron emission characteristics

A simple form of the neutron emission characteristics was assumed. The multiplicity of neutrons in generated events was taken form a Poisson distribution with the mean value, $< N_n >= 25$. This choice corresponds roughly to the neutron multiplicity distribution in a central heavy-ion collisions at intermediate energies; see e.g. ref. [39]. Energy distributions were taken from the Lund interferometry experiment ref. [13]; ($< E_n >= 12MeV$). Angular distributions were taken from the averaged experimental data in intermediate-energy heavy-ion collisions. The form of these distributions is presented in the Fig.16.

6.3 Statistics

The number of generated events was 1 000 000 for each considered detector configuration. The statistical data for all considered configurations are collected in Table 1. Analysis of the presented numbers leads to the following conclusions:

1. All the relations between the numbers of registered single particles, coincidences and cross-talks/diaphonies reflect well the general relations discussed above:

- the absolute number of cross-talk events decreases with the increase of the distance target-detectors but the number of coincidences ($N_n > 1$) decreases as well.
- comparison ot the results for TEST1 and TEST2 configurations shows that the ratio of cross-talk to coincidences does depend very little on the distance target-detector,
- in the case of the "Compact" configuration each second "coincidence" event is due to cross-talk,
- when the distance target-detector is approximately doubled - the number of coincidences decreases about 13 times.

2. The relative number of cross-talks increases with the decrease of the registration threshold.

3. The rate of cross-talks and diaphonies to the number of registered neutrons is small (about one percent). It is thus not important for inclusive characteristics.

4. With the increase of the distance target-detector the number of multiple registrations ($N_n > 1$) drastically decreases thus leading to a strong reduction of the possible two-particle combinations.

6.4 "Measured" correlation function

In the case of the standard DEMON configuration (Fig.13) the detectors are dispersed. This dimnishes the cross-talk effects but also makes it impossible to register small momentum differences between registered neutrons. The modified configuration allows to register small momentum differences but also increase the amount of cross-talks.

Fig. 17. demonstrates these dependences. In the standard configuration the number of cross-talk events is negligible but the correlation function is cut at 8 MeV/c. In the modified configuration the registration region starts from 2MeV/c giving much better statistics in the region of effect. In this case, however, the cross-talk contribution becomes visible and can influence the form of the measured correlation function. Note: the form of correlation function presented in this figure does not include the effects of cross-talks and diaphony.

Fig.18 a,b. show the generated and "measured" correlation function (a), and the distribution of the momentum differences (b), for the standard DEMON configuration. The value of the time parameter ($\tau_0 = 300 fm/c$) was choosen to reflect the time intervals expected in intermadiate energy heavy ion collisions. The "measured" correlation function has no points in the most interesting region of smallest momentum differences. For greater values of relative momenta the statistics is poor and the correlation function is deformed by the geometrical structure of the detector.

The opposite situation is found for the compact configuration (Fig.18 c,d). In this case almost all points are located in the region of effect but the number of cross-talk events for small momentum differences is many times greater than the number of registrated coincidences. A huge cross-talk peak in the region of smallest relative momenta makes it impossible to extract correlation function from the data.

The presentation of the other results will be proceeded by a short description of the method of cross-talk rejection as this approach was applied in the analysis of the simulated data.

6.5 The method and results of cross-talk rejection

Cross-talk is a spurious coincidence event in which the incident neutron deposits some energy in the first detector (being registered), and next do the same in the second one. These two acts of energy deposition and registration pass in well defined time sequence – the first detector "fires" first. It means that in the case of cross-talk, the energy measured by the time-of-flight technique will be always smaller in the second detector.

Let us consider a system of two detectors located in distances d_1 and d_2 from the target (Fig.19). The difference in distance is: $\Delta d = (d_2 - d_1)$. An example a) shows the most frequent cross-talk event; a neutron registered in the first detector is scattered forward and registered also in the second one. The distance-energy relation is:

$$\Delta E = (E_2 - E_1) < 0; \qquad sign\Delta E = -sign\Delta d. \tag{24}$$

whre E is the neutron energy determined by the time-of-flight method.

In the case b), where $d_1 = d_2$, this relation cannot be defined. In the case c), the relation is:

$$\Delta E = (E_2 - E_1) \gg 0; \qquad sign\Delta E = sign\Delta d. \tag{25}$$

The symbol " $\gg$ " indicate that in this case the energy difference is opposite and much greater than in the case a). First, it is due to the distance-energy relation (scattered neutron will be registered at smaller distance); and second, due to large energy degradation in the backward scattering. It is important for interferometry analysis that in this case the cross-talk event will be shifted to the region of larger momentum difference which is not so sensitive to the correlation effect and is better

populated by the real coincidences. Note also that the probability of cross talk is much smaller in the backward direction [14].

A cross-talk event of the type a), can be selected by the following condition:

$$S_{c-t} = (d_1 \neq d_2) \wedge (sign\Delta E = -sign\Delta d) \tag{26}$$

This condition should be checked for all two-detector combinations. If the value of the logical variable S_{c-t} is $true$, a cross-talk of type a) was detected. In other words, by accepting only the (n, n) pairs in which energy registered by the more distant detector is greater, all the cross-talk events from close to distant detectors will be removed. Of course, half of the coincidence events will be lost as well and this is the price for almost complete elimination of cross-talk events.

The relations discussed above are illustrated in Fig.20, where the dependence between Δd and ΔE is presented for the cross-talk events in the TEST1 configuration of the DEMON detector (see Fig.14). The maxima seen for the values of $|\Delta d|$ about 50cm and about 100cm corresponds to different combinations of detectors in the frame of the three-detector subsystem. The maxima for Δd=0 shows the cross-talk events between different systems of three detectors. This figure demonstrates well the main features of distance-energy dependences described above. Large maxima in the region defined by the condition (26) will be rejected by the removing procedure. Those, corresponding to the case c) are shifted in the energy scale and are of negligible statistics.

The presented scheme of cross-talk elimination can be somewhat improved by a more refined treatment. The relative angle between detectors, the value of neutron energy and the energy deposited in the detector can also be included in the distance-energy relations. In a limited interval of energy difference, some "cross-talk free" region can be selected even in the case of equal target-detector distances. This effect is seen in the Fig.20. as a minimum for the values of Δd and ΔE close to zero. The width of this region depends on the neutron energy and distance between detectors. Cross-talk events corresponding to d_1=d_2 cannot be removed but can be suppressed by a proper geometrical configuration. The alternated localisation of three-detector systems was choosen to diminish this effect. In a real experiment the detector response function should also be taken into account. A pulse shape analysis can give some supplementary information as well [12].

The distance-energy relations described above have been observed experimentally in the first neutron-neutron correlation measurement [9]. The asymmetry of the time-ot flight distributions was observed for the combination of detectors located at different distances from the target. In this experiment the background pairs were subtracted using the results of additional measurements with a "shadow-bar" in front of selected detectors.

Practical results of cross-talk rejection are shown in Fig.21. Left part demonstrates the correlation function obtained with full statistics of registered pairs. The measured correlated function is clearly above the generated one. The ratio of measured to generated correlation function shows a distinct deviation from the value of one. The rejection of cross talk gives satisfactory agreement between generated and measured correlation function.

7 Conclusions

1. The results of Monte-Carlo calculations demonstrate practical possibility to use the DEMON multidetector system for the measurenents of neutron-neutron correlations in the region of small momentum difference.

2. In order to perform an effective interferometry measurement, the geometrical configuration of the DEMON modules should be arranged in such a way that makes it possible to measure small relative angles between registered neutrons and allows to eliminate the spurious coincidence events (cross-talk).

3. A simple method allowing to remove the cross-talk events is proposed and checked by the Monte-Carlo simulations.

4. A simultaneous measurement of correlations for different two-particle systems is highly desirable in order to develop a consistent theoretical description of the experimental results.

5. In order to perform a complete interferometry experiment with the system of two nucleons the DEMON-detector should be equipped with a system of detectors for charged particle registration.

References

[1] M.I.Podgoretsky, Elementary Particles and Atomic Nuclei, **20**, No.3, 628, Dubna (1989).

[2] D.H. Boal, C.K. Gelbke, B.K. Jennings, Intensity Interferometry in Subatomic Physics, Review of Modern Physics, **62**, No.3, (1990).

[3] G.I. Kopylov, M.I. Podgoretsky, Yad.Fiz. **15**, 392 (1972), **18**, 656 (1973), **19**, 434 (1994).

[4] S.E. Koonin, Phys.Lett. **70 B**, 43 (1977).

[5] R. Lednicky, V.L. Lyuboshitz, JINR, **E2-81-453**, Dubna (1981), Yad.Fiz. **35**, 1316 (1982).

[6] D.H.Boal, J.C.Shillcock, Phys.Rev. **C 33**, 549 (1986).

[7] S.Pratt, M.B.Tsang, Phys.Rev. **C 36**, 2390 (1987)

[8] S. Mrówczyński, Phys.Lett., **B 227**, 43 (1992).

[9] Yu.D. Bayukov et al., preprint **ITEP-127**, Moscow, (1984).

[10] Yu.D.Bayukov et al., Phys.Lett. **B 189**, 291 (1987).

[11] B.Jakobsson et al., Phys.Rev., **C 44**, R1238 (1991).

[12] R. Gentner et al., Z.Phys. **A 343**, 401 (1992).

[13] M. Cronqvist et al., Phys.Lett., **B 317**, 505 (1993).

[14] M. Cronqvist et al., Nucl.Instr. and Meth., **A317**, 273 (1992).

[15] S.E.Arnell et al., Nucl.Instr. and Meth., **A300**, 303 (1991).

[16] B.Heusch, Second IN2P3-RIKEN Symposium on Heavy-Ion Collisions, Obernai,France, April 9-12, 1990, 239 (1990)

[17] A.B. Migdal, Zh.E.T.F, **28**, 10 (1955).

[18] V.L. Lyuboshitz, Yad.Fiz. **48**, 1501 (1988) (SJNP, **48**, 956 (1988)).

[19] P.Danielewicz, P.Schuck, Phys.Lett., **B 274**, 268 (1992)

[20] N.Angelov et al., Yad.Fiz., **32**, 1357 (1980).

[21] J.Bartke et al., Z.Phys., **A 324**, 471 (1986).

[22] M.L.Allaberdin et al., Yad.Fiz., **46**, 1785 (1987).

[23] J.Pochodzalla et al., Phys.Rev. **C 35**, 1695 (1987).

[24] W.Dunnweber et al., Phys.Rev.Lett. **65**, 297 (1990).

[25] R.A.Kryger et al., Phys.Rev.Lett. **65**, 2118 (1990).

[26] M.A.Bernstein, W.A.Friedman, W.G.Lynch, Phys.Rev. **C 29**, 132, (1984).

[27] R.A.Kryger et al., Phys.Rev. **C 46**, 1887 (1992).

[28] A.Elmaani et al., Comput.Phys.Commun. **59**, 507 (1990).

[29] W.G.Gong et al., Phys.Rev. **C 45**, 363 (1992).

[30] W.Gong, W.Bauer, C.K.Gelbke, S.Pratt, Phys.Rev. **C 43**, 781 (1991).

[31] S.Yu Kun, R.Gentner, L.Lassen, Z.Phys. **A 342**, 67 (1992).

[32] G.Bertsch, P.Danielewicz, H.Schulz, Europhys.Lett. **21**, 817 (1993).

[33] B.Erazmus et al., Phys.Rev. **C 49**, 349 (1994).

[34] J.M.Alexander et al., Phys.Rev. **C 48**, 2874 (1993).

[35] R.Lednicky et al. in preparation.

[36] A.Kugler et al., Proc of the Int.Workshop on Gross Properties of Nuclei and Nuclear Excitations, XX, January 20-25 (1992).

[37] P. Desesquelles et al., Nucl.Instr. and Meth., **A 307**, 366 (1991).

[38] Comite d'experiences, December 1993, **GANIL R 93 14**, 26, 73 (1993).

[39] D.X.Jiang et al., Nucl.Phys. **A 503**, 560 (1989)

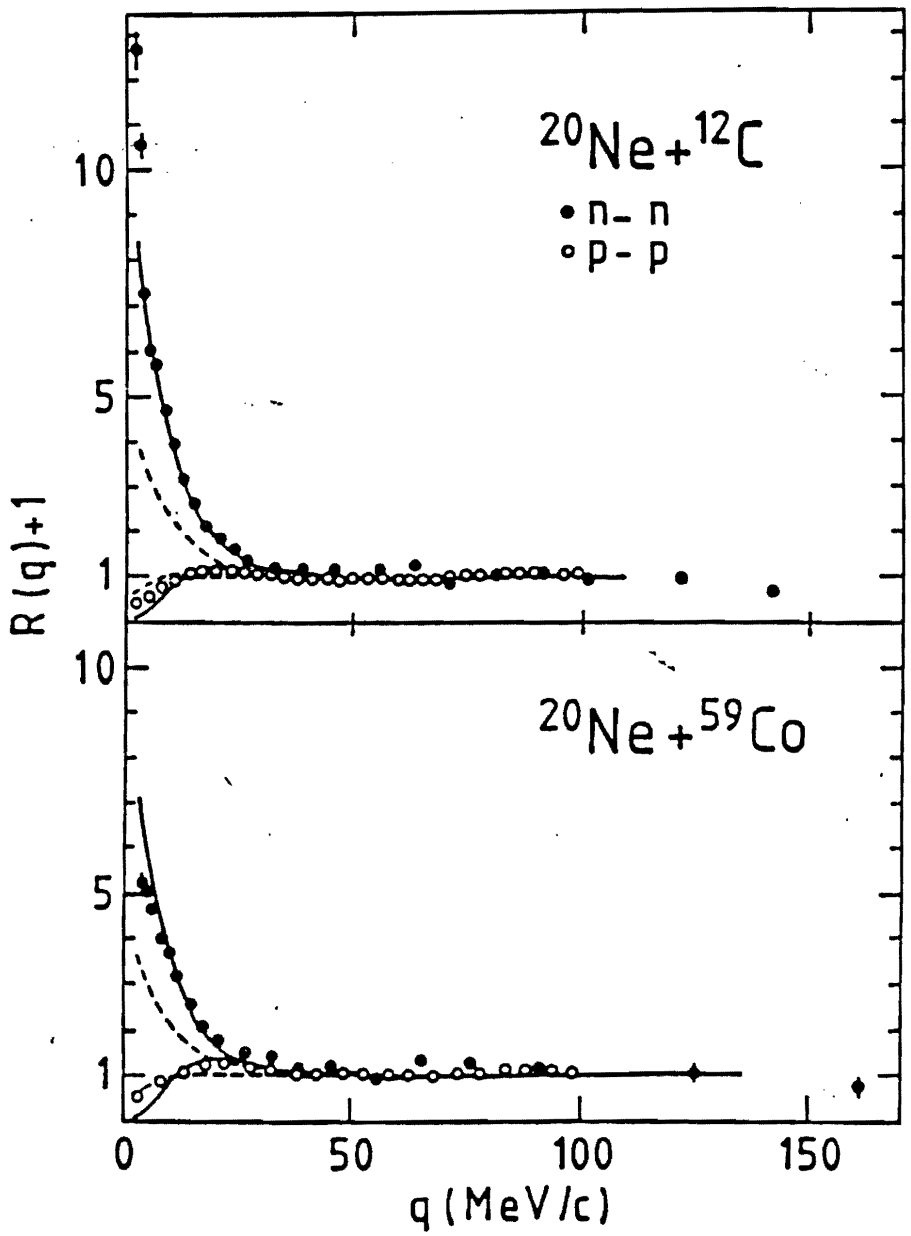

Correlation functions for *p-p* and *n-n* correlations in ^{20}Ne+C reactions (upper) and ^{20}Ne+Co reactions (lower) at 30*A* MeV. The solid curves come from a $\Delta\tau = 0$ interferometry calculation [22] where the source size is set to 5.0 fm. The dashed curves come from a fusion-evaporation calculation.

Fig.1. Correlation functions for (n,n) and (p,p) pairs. (from ref.[11])

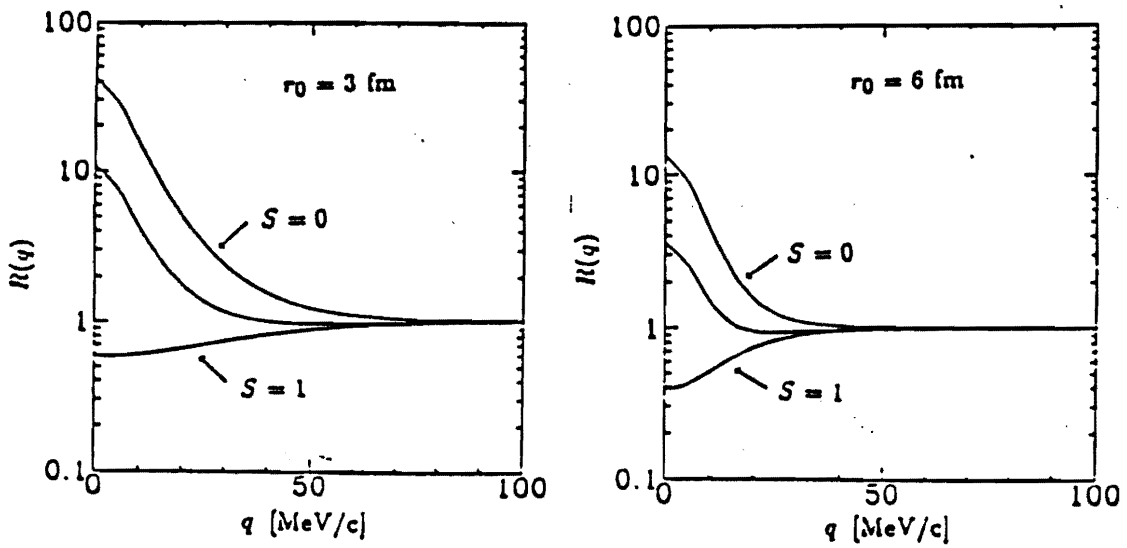

Fig.2. The singlet,triplet and spin average n-p correlation function versus q at $v\tau$=0. The values of r_0 are: 3fm (left) and 6fm (right). (from ref. [8])

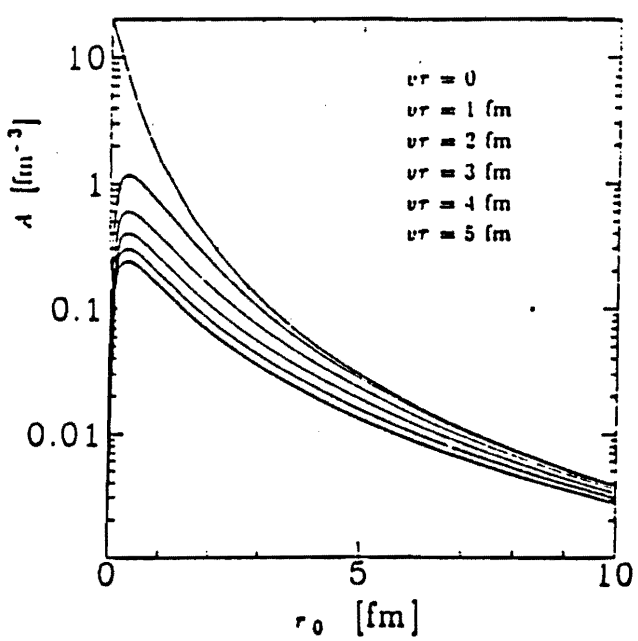

Fig. 1. The deuteron formation rate as a function of r_0 for several values of $v\tau$. The value of $v\tau$ increases from the highest line ($v\tau$=0) to the lowest line ($v\tau$=5 fm).

Fig.3. The deuteron formation rate can be used to find the space-time parameters of the emission process. (from ref. [8])

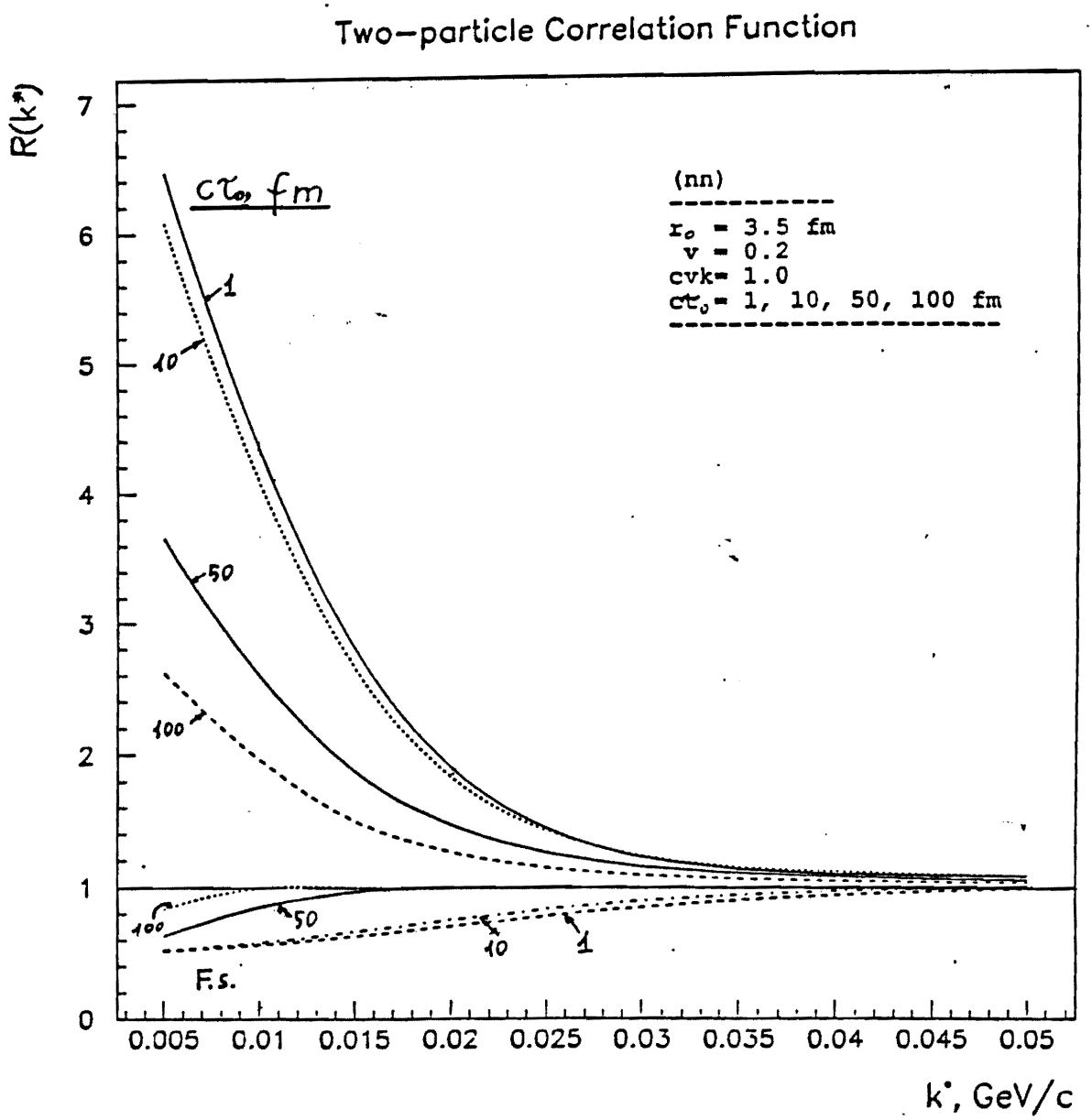

Fig.4. Neutron-neutron correlation functions for different values of the time parameter, τ. The Gaussian-like space-time distribution of the emitting points was assumed: r_0 - space parameter, v - pair velocity, cvk - $\cos(\vec{v}, \vec{k}^*)$, F.s. - correlation function for the effect of Fermi-statistics only.

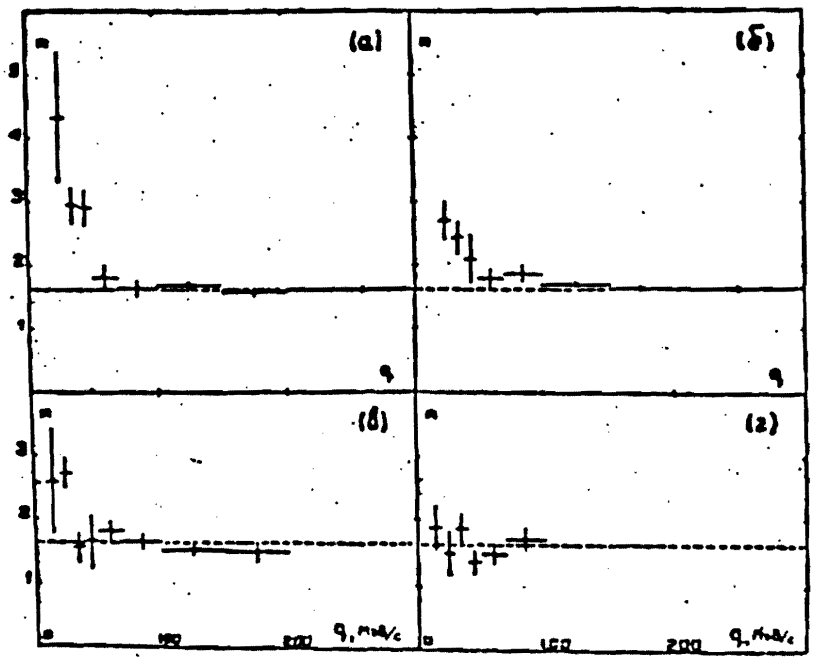

Fig.5. The first experimental correlation distributions for (n,n) pairs obtained at ITEP, Moscow in 1984. Correlation effect decreases with decreasing value of neutron energies. (from ref. [9]).

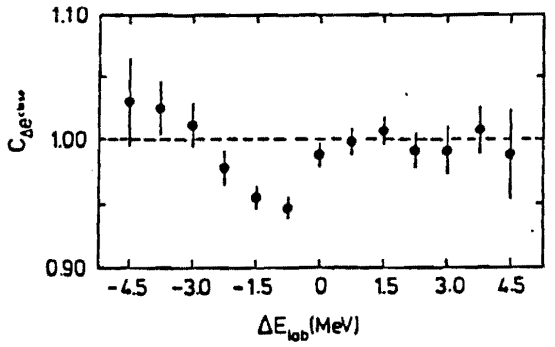

FIG. 3. Correlation function [Eq. (3)], averaged over both experiments, as a function of the energy difference $\Delta E_{lab} = E_{lab}(\theta_2) - E_{lab}(\theta_1)$ for neutrons with $E_{lab} = 3$–8 MeV.

Fig.6. (above) Correlation function for (n,n) pairs emitted in the reactions $^{18}O + {}^{26}Mg \rightarrow {}^{44}Ca$, ($E_x = 60$ and 71 MeV). (from ref. [24])

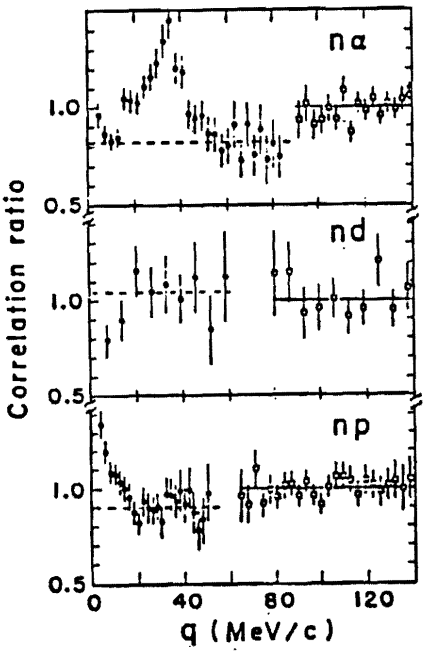

FIG. 1. Correlation functions for *na*, *nd*, and *np* coincident events. Small-opening-angle data are indicated by circles and large-opening-angle data by squares. The dashed and solid horizontal lines indicate the background correlation ratio for the small- and large-opening-angle data as explained in the text.

Fig.7. (right) Correlation function for (n,p) pairs emitted in the reaction $^{16}O + {}^{27}Al$ at $E(^{16}O)$=215MeV. (from ref.[25])

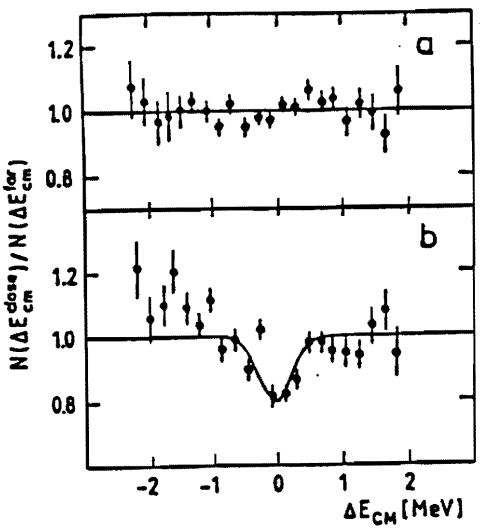

Fig. 5a, b. Experimental correlation function (3) vs. neutron energy difference ΔE_{cm}. a For uncorrelated neutron pairs obtained by event mixing from the same class of events, taking random energy values from the spectra in close and far geometry, respectively, and b for true coincidences. For comparison, the solid curve in panel b denotes a gaussian distribution with half width (FWHM) of 600 keV (average experimental energy resolution)

Fig.8. Correlation function for (n,n) pairs emitted in the reaction $^{18}O +^{64} Ni$ at 96 MeV. (from ref. [12])

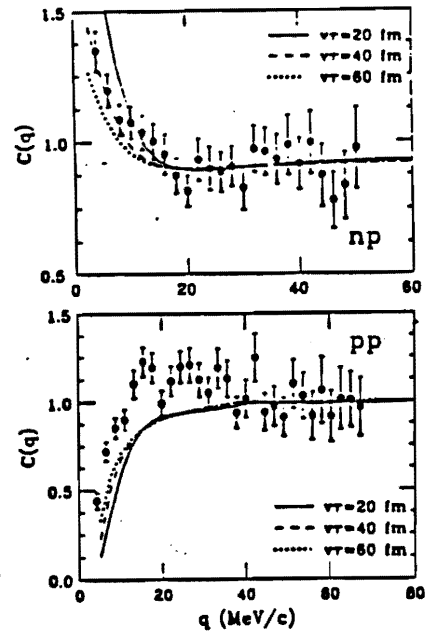

FIG. 8. *np* and *pp* small-angle correlation data compared with correlation functions calculated with the Koonin model. The different calculations correspond to different source sizes.

Fig.9. Correlation function for (n,p) and (p,p) pairs emitted in the reaction $^{16}O +\ ^{27}Al$ at $E(^{16}O)$=215MeV. (from ref. [27])

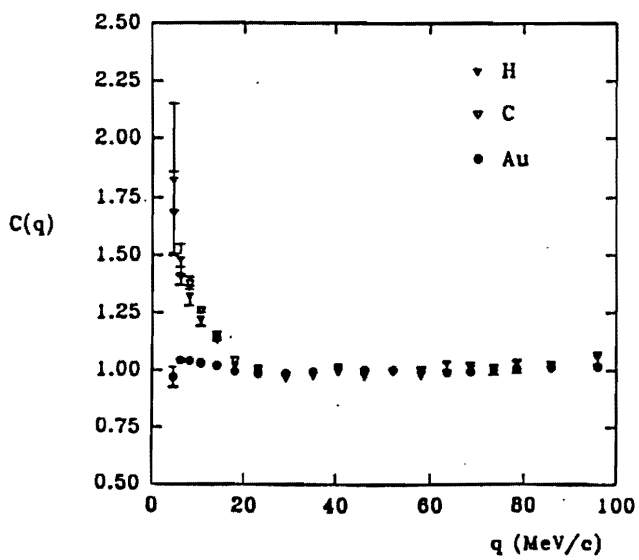

Fig. 2. Experimental np correlation functions for Ar+Au, Ar+C and Ar+H reactions.

Fig.10. Correlation functions for reactions: $^{40}Ar +\ ^{191}Au$, ^{12}C, CH_2 at 30 MeV/u. (from ref.[13]).

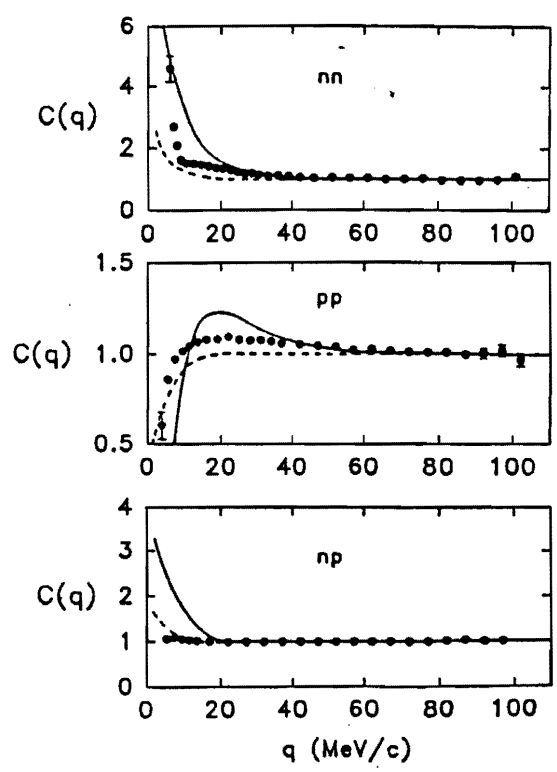

Fig. 1. Experimental nn, pp and np correlation functions at 45° from 30*A* MeV Ar+Au collisions compared to calculated functions from a pure evaporative approach (dashed curves) and a BUU pre-equilibrium approach (solid curves).

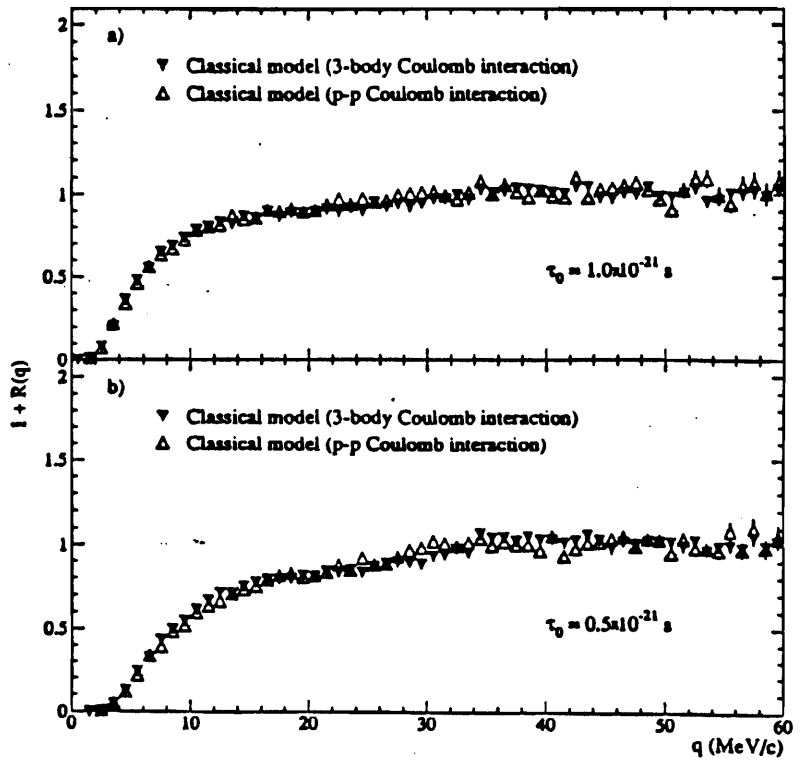

FIG. 6. Predictions of classical calculations for p-p correlation function with and without treatment of the interaction with the emitting nucleus for (a) $\tau_0 = 10^{-21}$ s and (b) $\tau_0 = 5\times10^{-22}$ s.

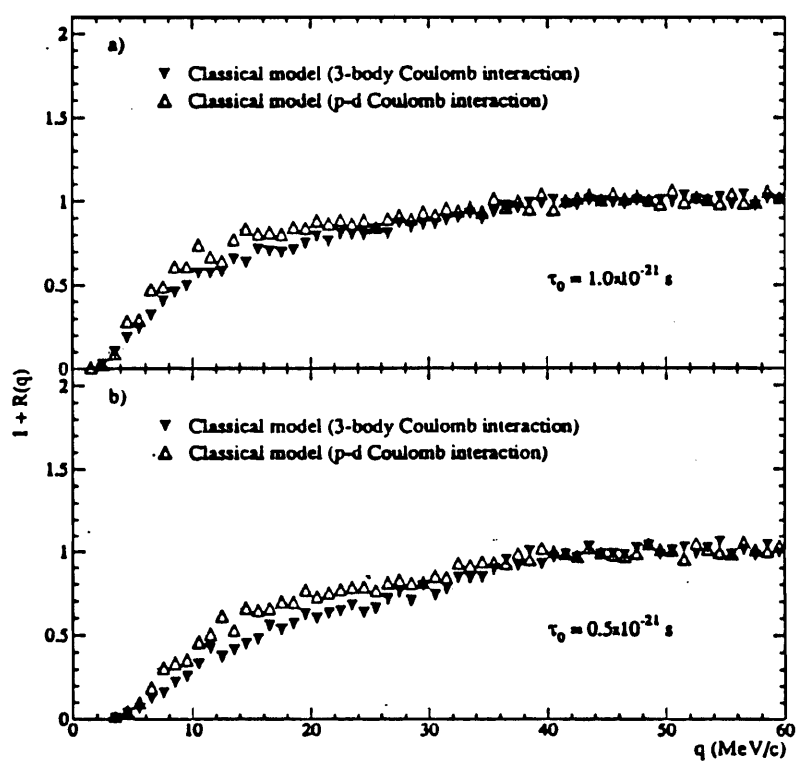

FIG. 7. Same as Fig. 6 for proton-deuteron correlation function.

Fig.11. Results of two, and three-body clasical calculations for (p,p) - upper figure, and (p,d) - lower figure. (from ref.[33])

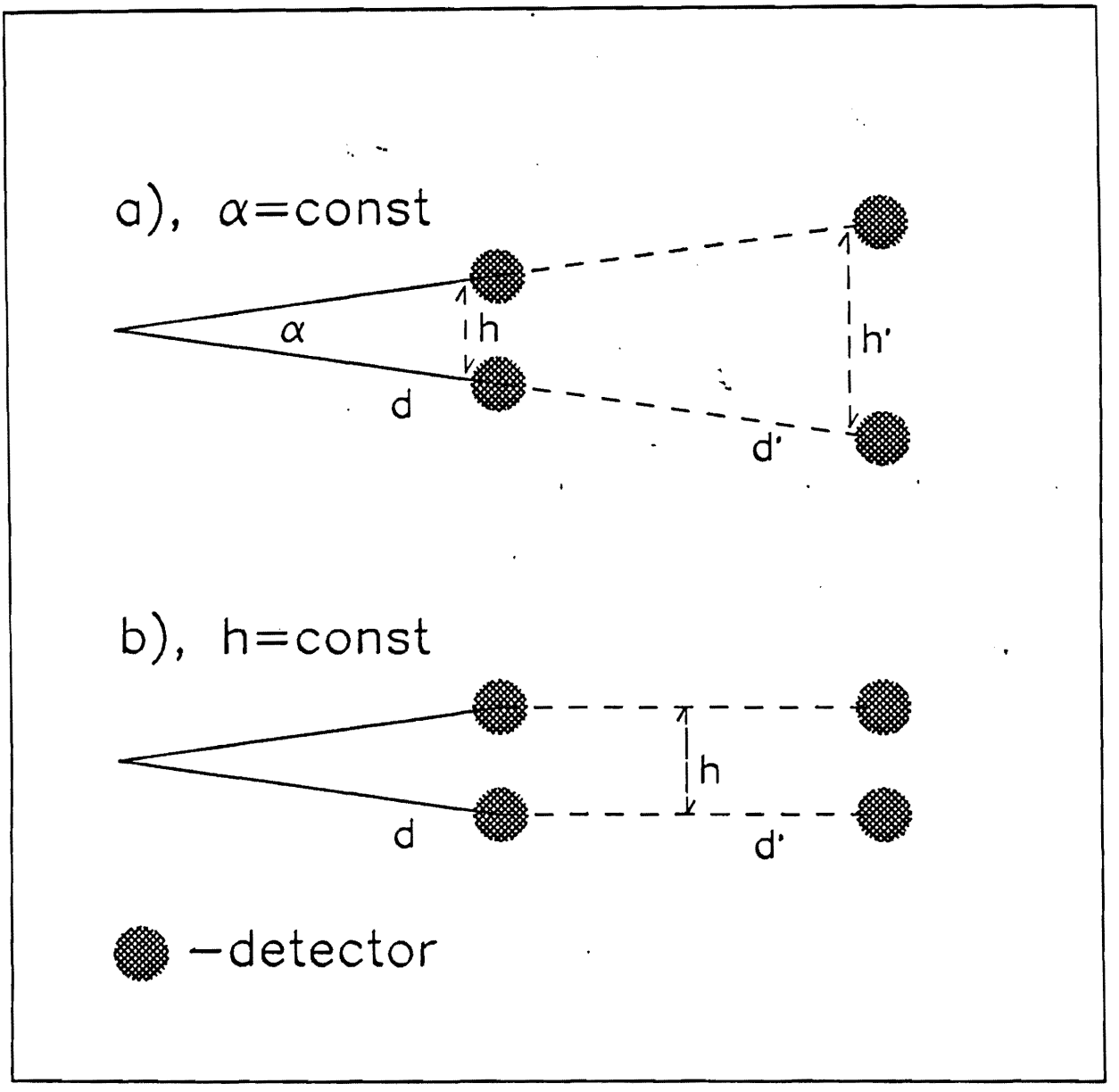

Fig.12. Probability relations between cross-talk and coincidences.

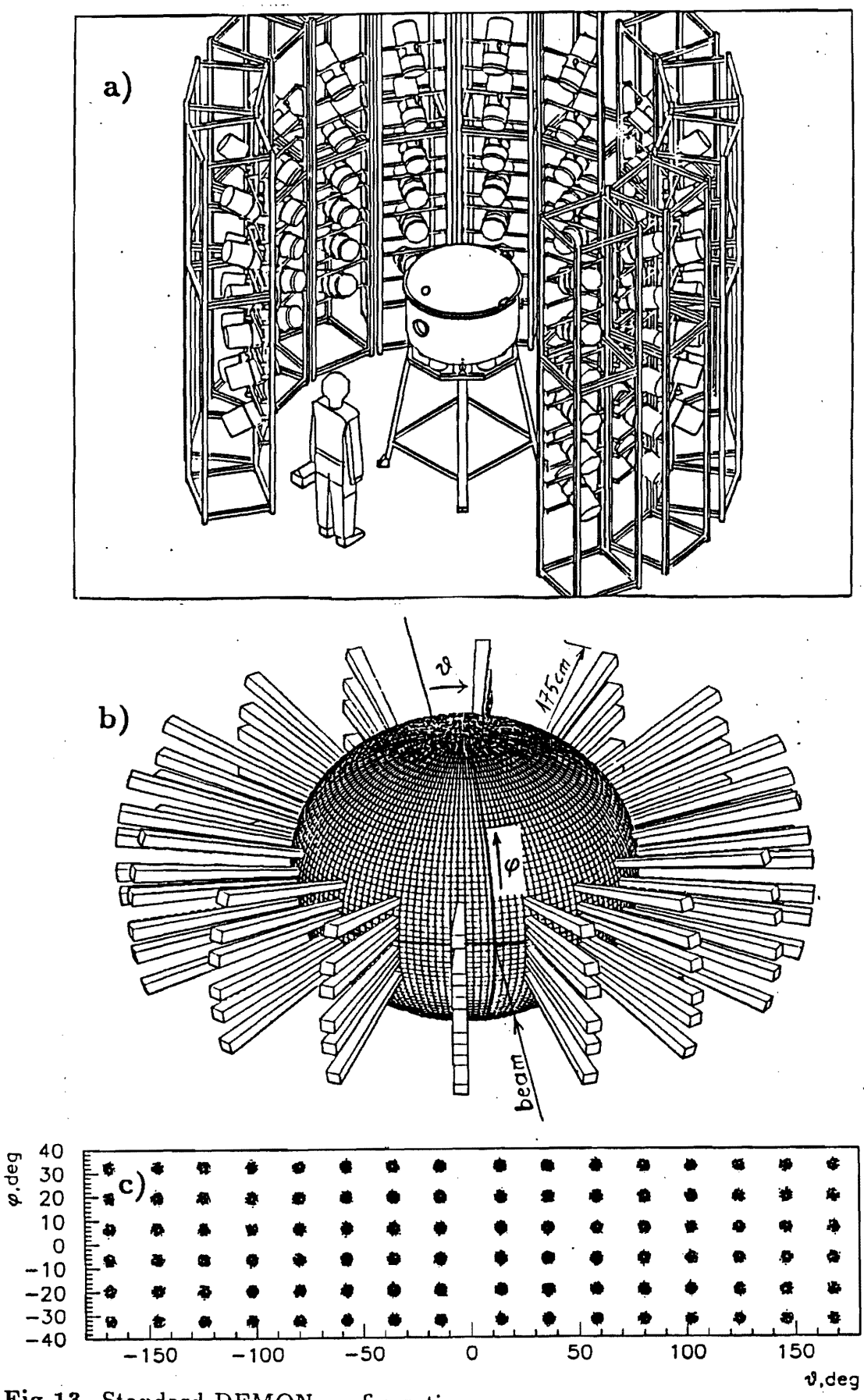

Fig.13. Standard DEMON configuration:
a) -perspective view from ref. [38]
b) - schematic diagram of geometrical configuration,
c) - angular distribution of the neutron hit-positions at the surface of detectors for 20 000 generated events.

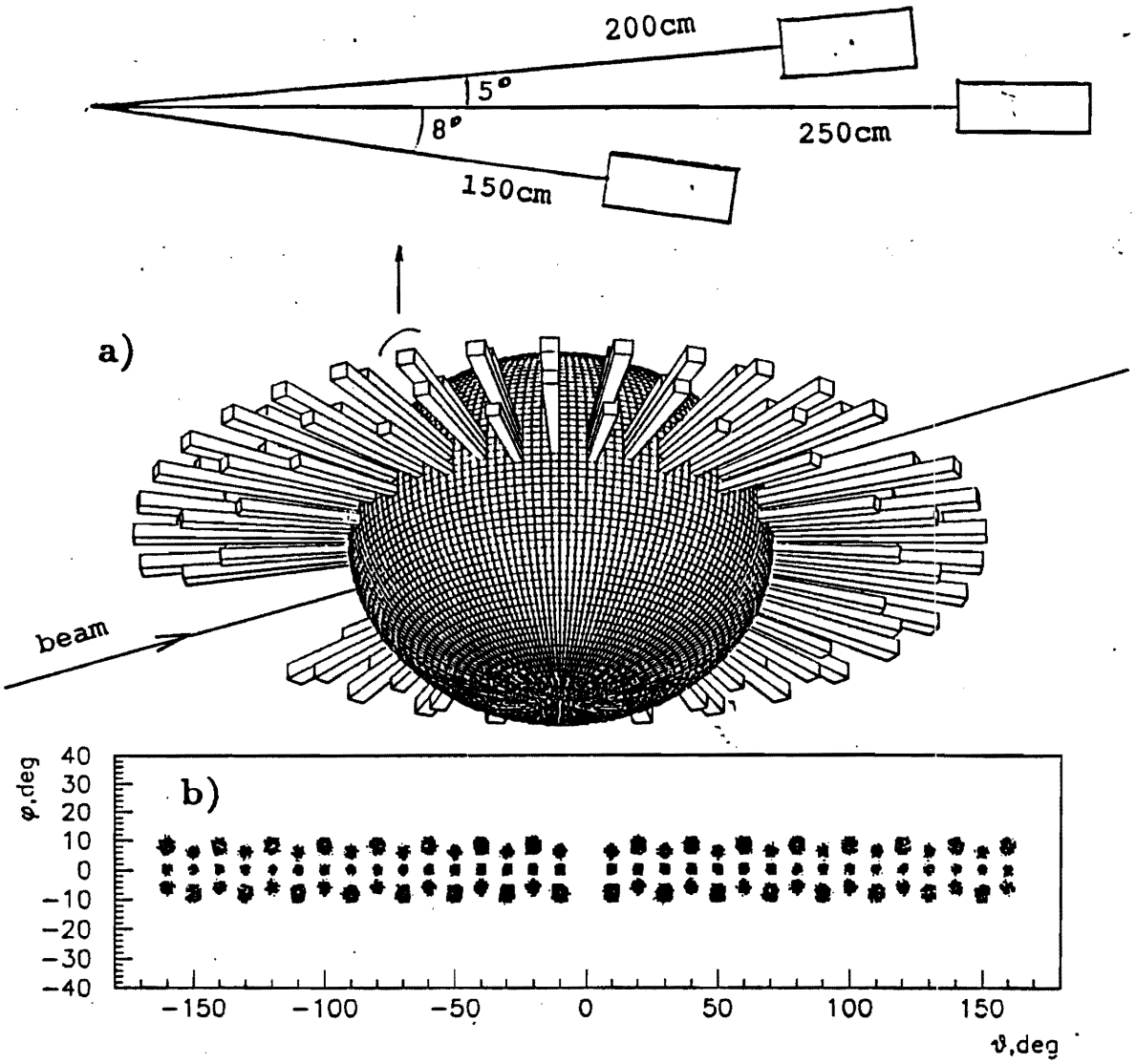

Fig.14. Modified DEMON configuration: a) - schematic viw, b) - angular distribution of hit-positions at the surface of detectors for 20 000 events.

Fig.15. Compact DEMON configuration:
a) schematic view,
b) hit positions for 200 000 events.

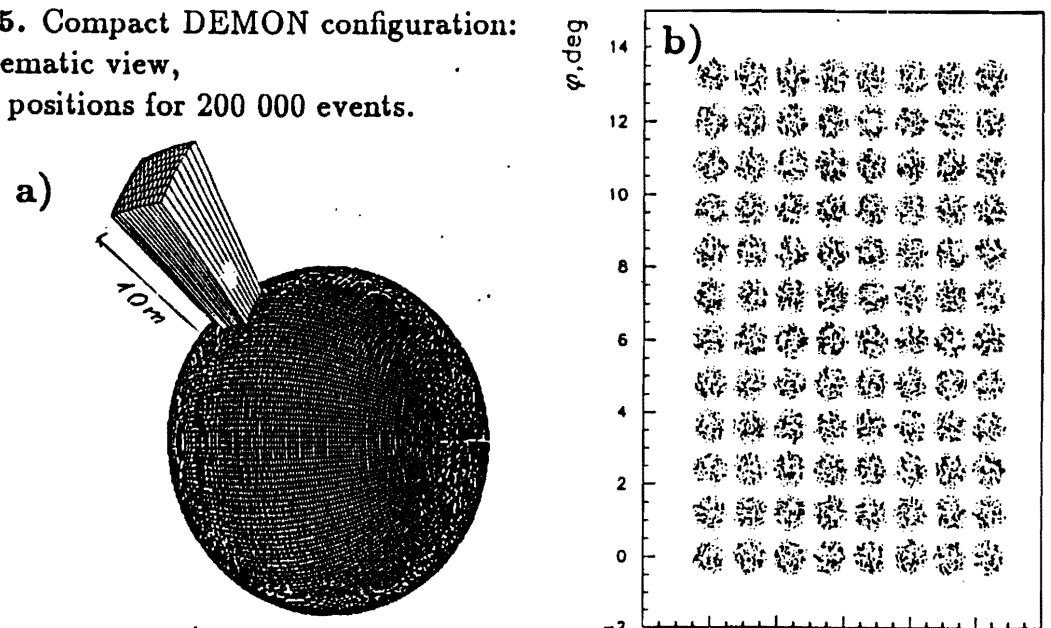

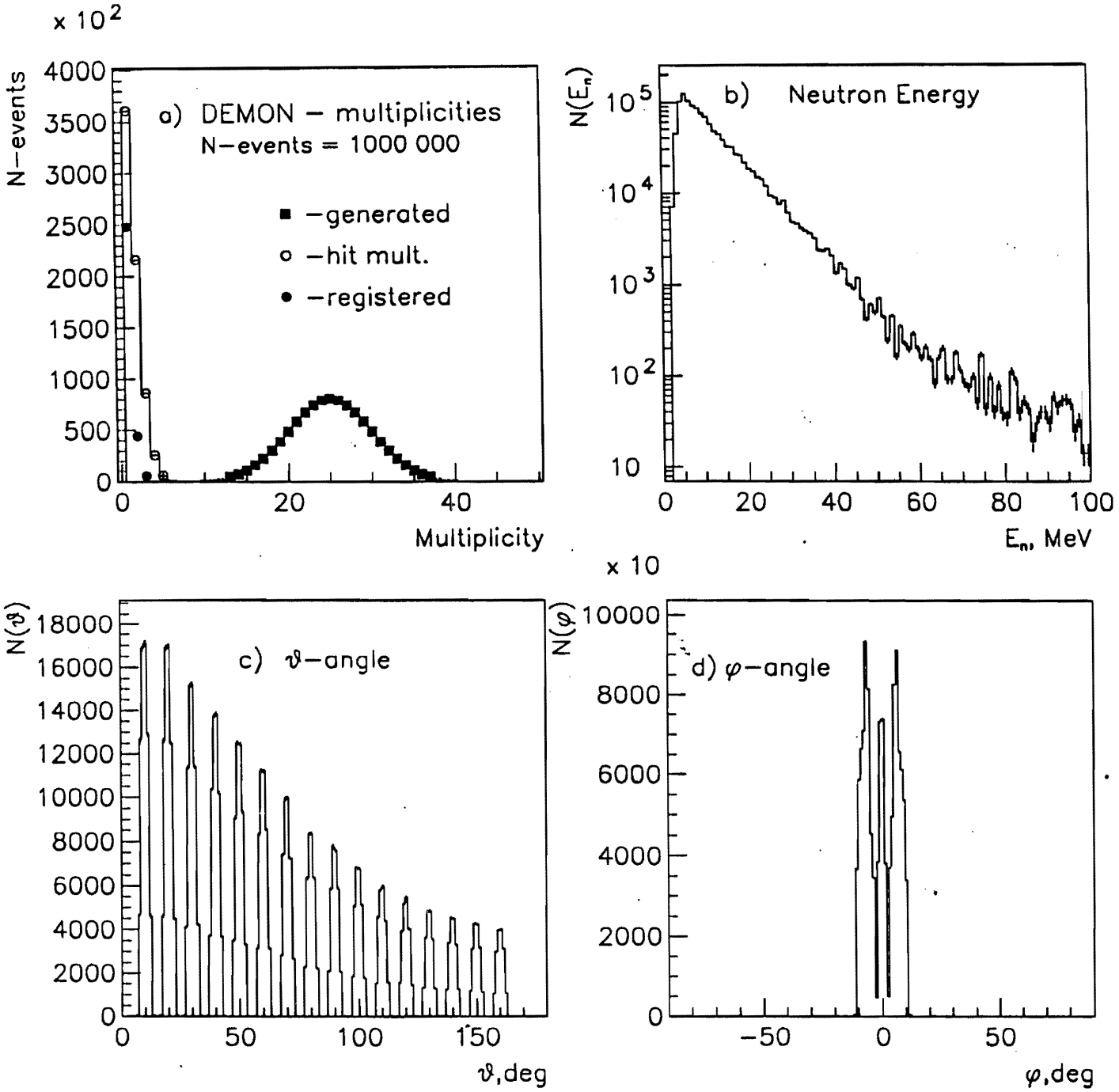

Fig.16. Main characteristics of generated neutrons for 1 000 000 events registrated in modified DEMON configuration, TEST1:
a) - multiplicity distribution,
b) - energy distribution,
c) - horizontal angle distribution,
d) - vertical angle distribution.

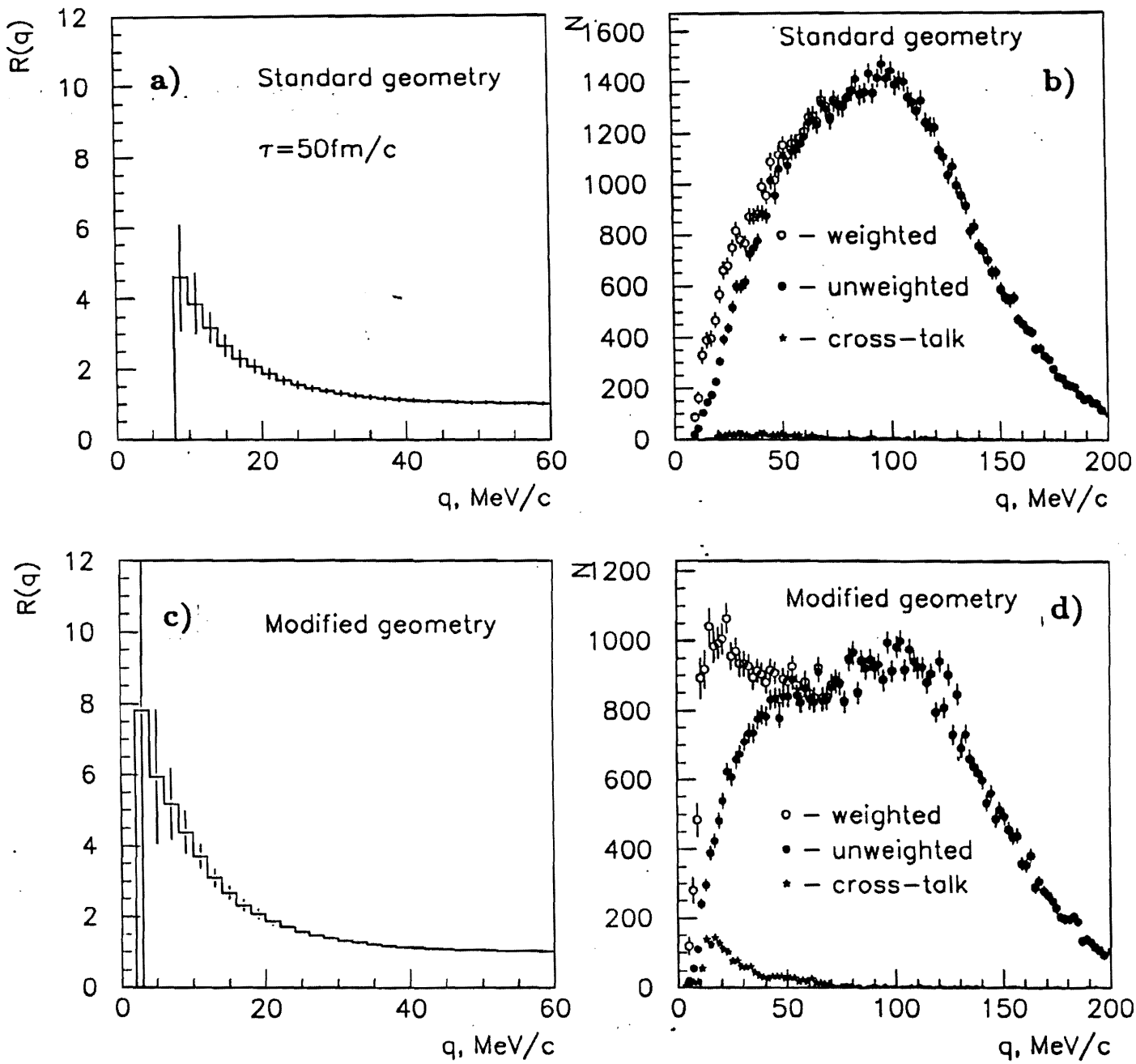

Fig.17. Correlation characteristics for the Standard and Modified configurations of the DEMON detector.
a), c) - undistorted correlation function for $\tau_0 = 50 fm/c$.
b), d) - distribution of the neutron momentumm differences. Correlation function is defined as a ratio of weighted to unweighted distributions.

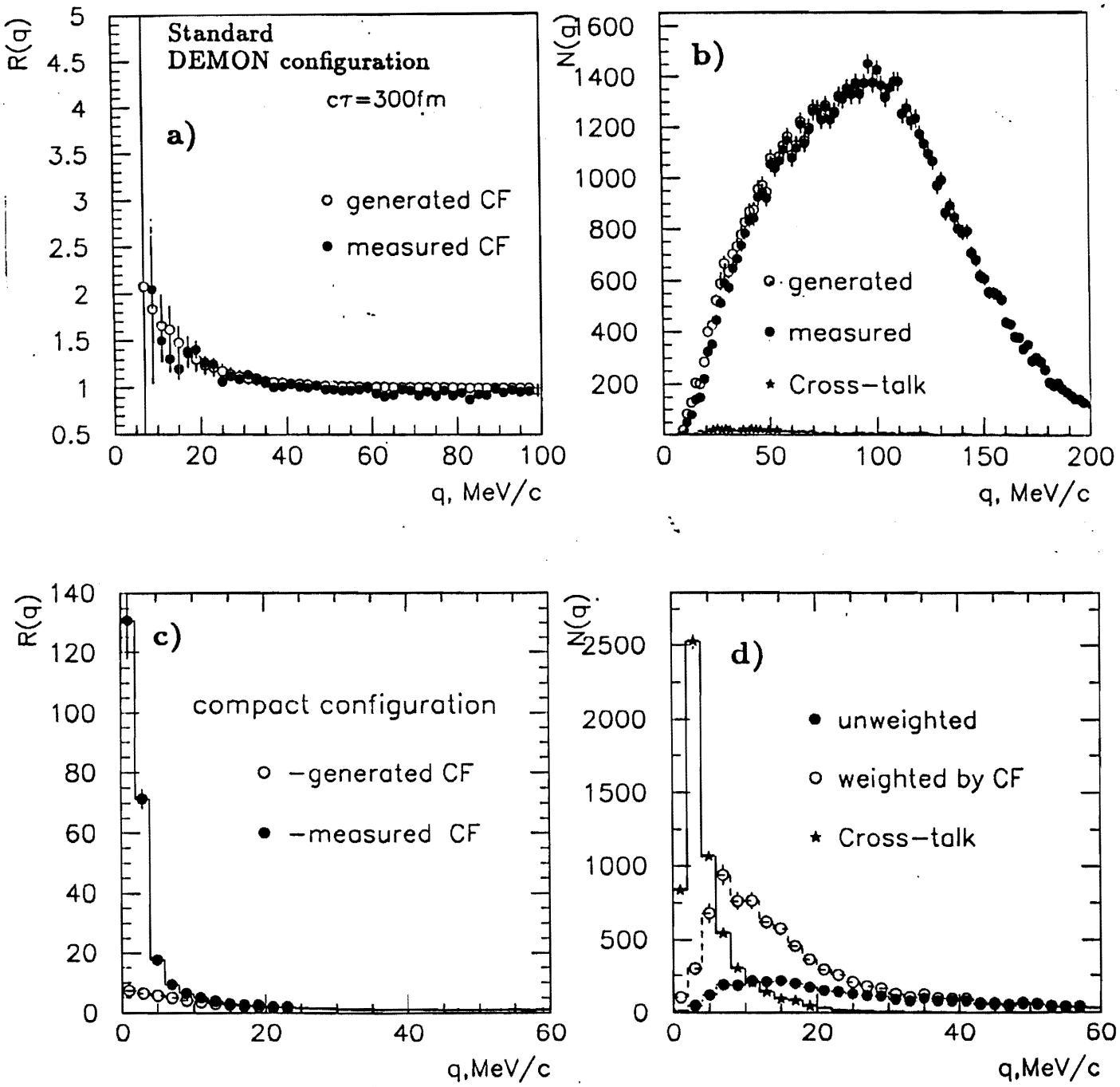

Fig.18. Correlation functions (left) and distributions of momentum difference (right) for the standard (upper) and compact (lower) configurations of the DEMON detector.

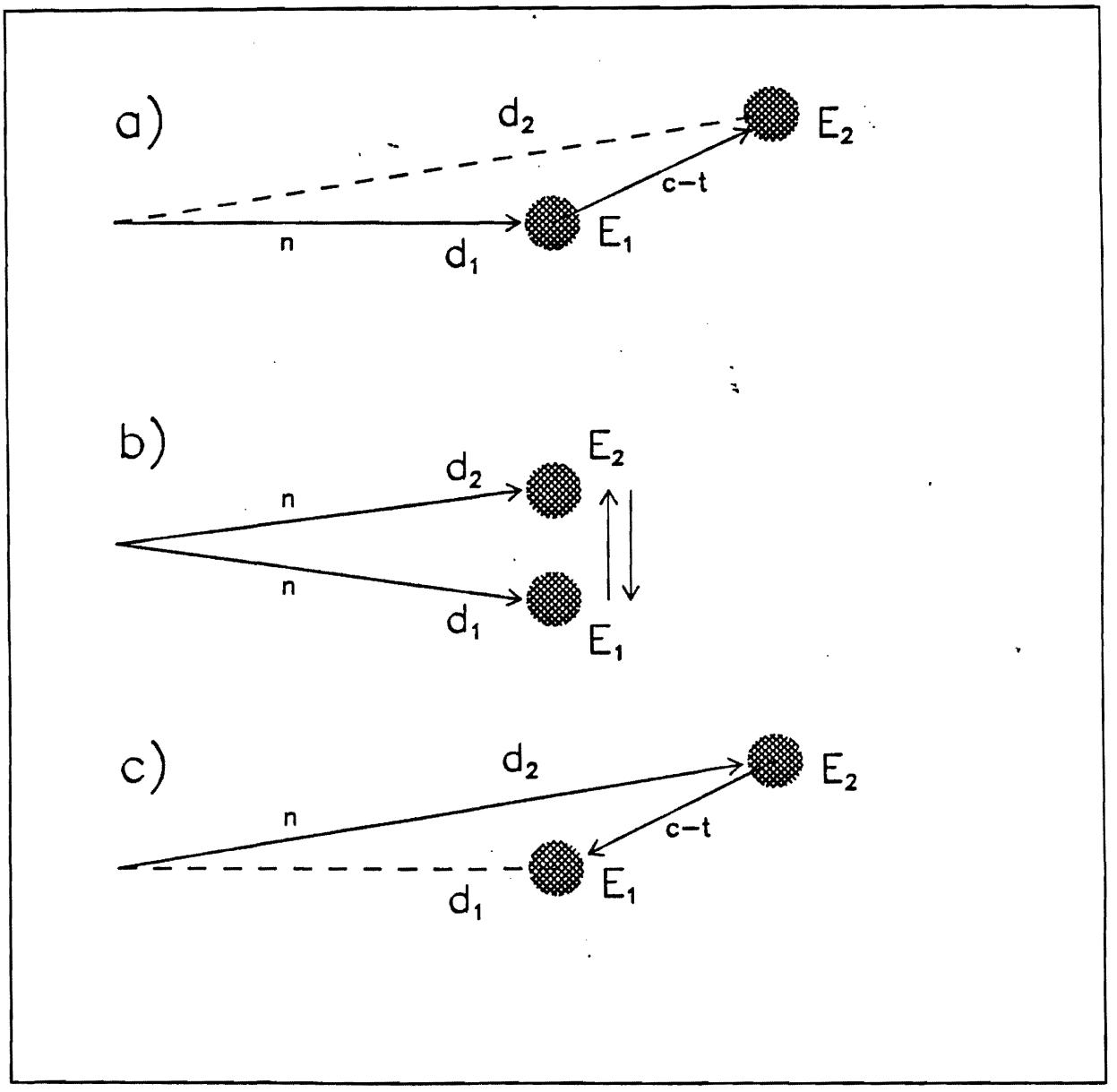

Fig.19. Distance-energy relations for cross-talk events.
a) - cros-talk from close to distant detector; ($E_2 < E_1$),
b) - both detectors are in equal distance from the target,
c) - cross-talk from distant to close detector; ($E_2 \gg E_1$).

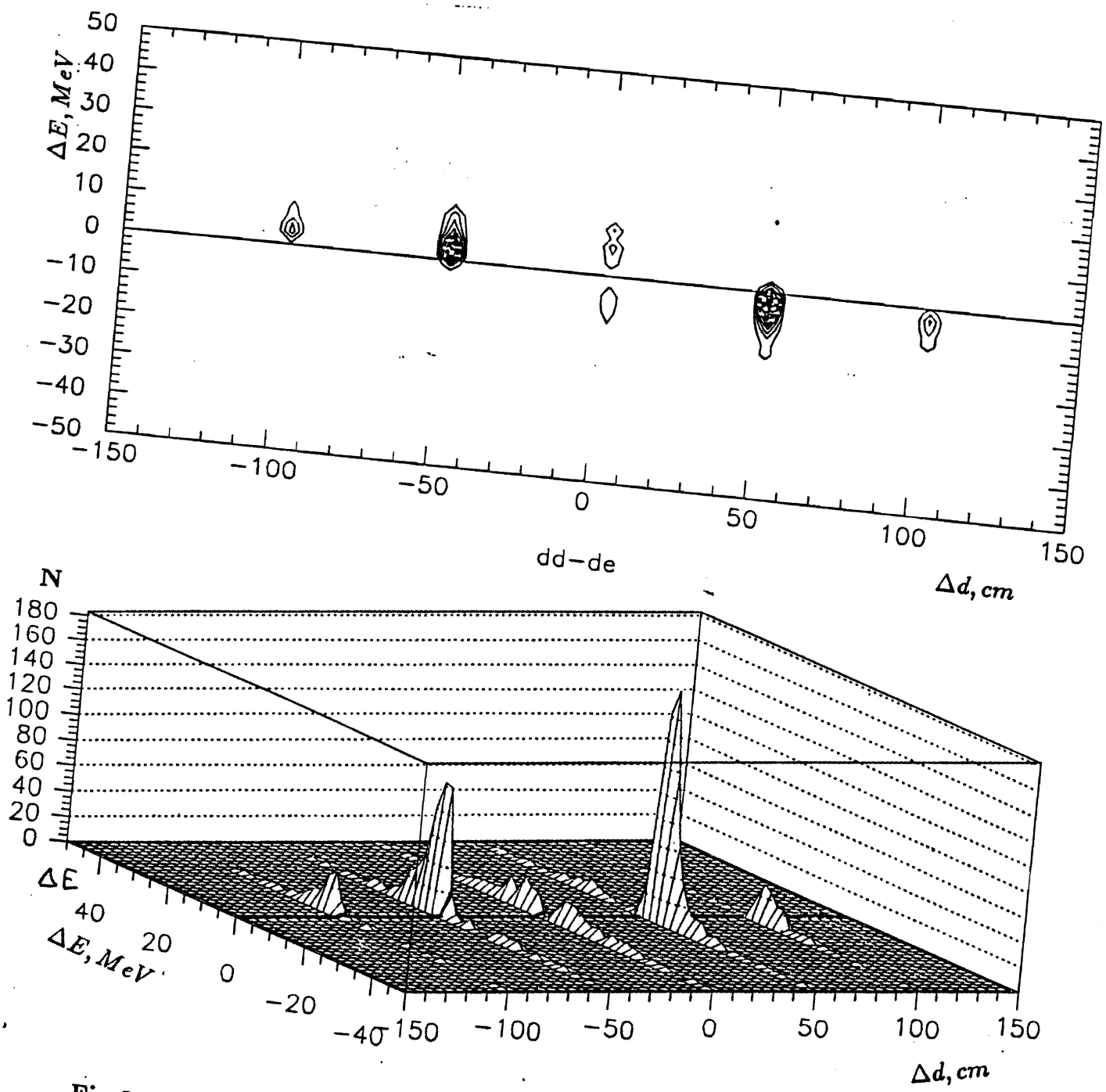

Fig.20. Cross-talk rejection method. All the points defined by the relation: $sign\Delta E = -sign\Delta d$ will be removed. See text for explanations.

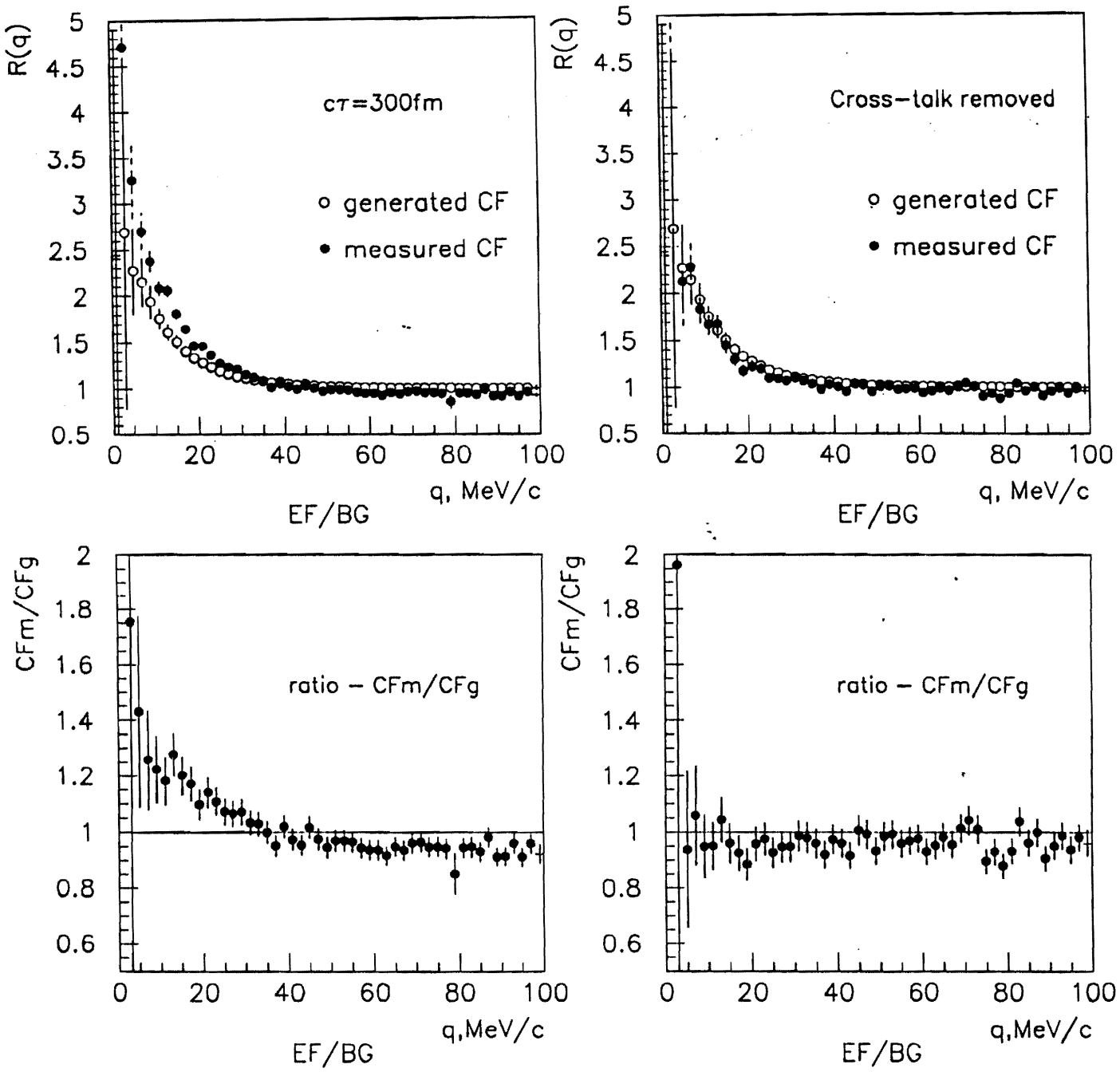

Fig.21. Correlation function measured in the modified DEMON configuration, TEST1, with different distances between target and detector. Left side - all registered pairs (including cross-talks); right side - after rejection of cross-talk events.

Table 1.

STATISTICS OF NEUTRON REGISTRATION BY THE "DEMON" DETECTOR

(Data for 1000 000 collisions for each detector configuration)

A	configuration	E240exp.	TEST1	TEST2	compact	TEST1,a
B	distance,cm	175	150,200,250	350,400,450	1000	150,200,250
C	det. hits	1 291 442	1 191 285	298 991	74 913	1 191 285
D	registrated	391 999	350 313	91 234	23 860	536 145
E	cross-talks	713	1 804	137	489	8 424
F	diaphonies	2905	3 607	861	2 709	6 371
G	(E+F)/D	0.0092	0.0154	0.0101	0.134	0.0276
H	Nev(Nn>1)	60 341	50 309	4 045	868	107 931
I	E/H	0.0118	0.0358	0.0331	0.563	0.078
J	Hit mult.					
	1	354 587	361 595	221 730	69 516	361 595
	2	229 292	215 696	33 165	2 602	215 696
	3	98 863	85 783	3 300	64	85 783
	4	31 919	25 534	243		25 534
	5	8 212	6 053	12		6 053
	6	1 745	1 181			1 181
	7	308	186			186
	8	40	20			20
K	Reg. mult					
	1	266 536	248 447	84 014	25 294	311 961
	2	52 723	44 411	3 923	841	88 079
	3	6 908	5 492	118	26	16 991
	4	670	455	4		2 521
	5	36	27			317
	6	4	4			24
	7					5

A - The details of detector configurations are explained in the text.

B - distance between target and detectors,

C - number of neutrons which have hit the detectors,

D - number of registered neutrons,

E - number of "cross-talks",

F - number of "diaphonies",

H - number of events with two or more registered neutrons,

J - multiplicity distribution of hit detectors,

K - multiplicity distribution of registered neutrons,

(Neutrons are emitted with the Poisson distribution; <Nn>=25.)